Available online at www.sciencedirect.com
ScienceDirect
Journal of Solid State Chemistry 180 (2007) 2877–2884
JOURNAL OF SOLID STATE CHEMISTRY
www.elsevier.com/locate/jssc

$Cs_4P_2Se_{10}$: A new compound discovered with the application of solid-state and high temperature NMR

Matthew A. Gave[a], Christian G. Canlas[a], In Chung[a,b], Ratnasabapathy G. Iyer[a], Mercouri G. Kanatzidis[a,b,1], David P. Weliky[a,*]

[a]*Department of Chemistry, Michigan State University, East Lansing, MI 48824, USA*
[b]*Department of Chemistry, Northwestern University, Evanston, IL 60208, USA*

Received 2 May 2007; received in revised form 31 July 2007; accepted 5 August 2007
Available online 23 August 2007

Abstract

The new compound $Cs_4P_2Se_{10}$ was serendipitously produced in high purity during a high-temperature synthesis done in a nuclear magnetic resonance (NMR) spectrometer. ^{31}P magic angle spinning (MAS) NMR of the products of the synthesis revealed that the dominant phosphorus-containing product had a chemical shift of −52.8 ppm that could not be assigned to any known compound. Deep reddish brown well-formed plate-like crystals were isolated from the NMR reaction ampoule and the structure was solved with X-ray diffraction. $Cs_4P_2Se_{10}$ has the triclinic space group $P\bar{1}$ with $a = 7.3587(11)$ Å, $b = 7.4546(11)$ Å, $c = 10.1420(15)$ Å, $\alpha = 85.938(2)^\circ$, $\beta = 88.055(2)^\circ$, and $\gamma = 85.609(2)^\circ$ and contains the $[P_2Se_{10}]^{4-}$ anion. To our knowledge, this is the first compound containing this anion that is composed of two tetrahedral (PSe_4) units connected by a diselenide linkage. It was also possible to form a glass by quenching the melt in ice water, and $Cs_4P_2Se_{10}$ was recovered upon annealing. The static ^{31}P NMR spectrum at 350 °C contained a single peak with a −35 ppm chemical shift and a ~7 ppm peak width. This study highlights the potential of solid-state and high-temperature NMR for aiding discovery of new compounds and for probing the species that exist at high temperature.

Keywords: NMR; Solid state; High temperature; Chalcogenides; Metal selenophosphates; Phosphorus; ^{31}P

1. Introduction

Chalcophosphates are compounds with oxidized phosphorus and at least one P–Q bond, where Q = S, Se, or Te. These compounds exhibit an impressively rich structural diversity because of the large number of stable $[P_xQ_y]^{z-}$ building blocks that can be stabilized and the variety of binding modes in which they can engage [1]. They are important in the areas of catalysis, ceramics, glasses, and molecular sieves [2–4]. Previously, solid-state nuclear magnetic resonance (NMR) has been useful in providing structural information about chalcophosphate materials [5–10]. Most notably, in selenophosphate materials there is a general correlation between the chemical shifts (CSs) of anions and the presence or absence of a P–P bond. Compounds containing a P–P bond resonate between 25 and 95 ppm whereas those that do not contain a P–P bond resonate between −115 and 5 ppm [11]. Additionally, the spectral intensity of a peak in an NMR spectrum is proportional to the number of nuclei that have the corresponding chemical environment [12]. Therefore, NMR spectroscopy is a useful tool to evaluate phase purity in cases where competing compounds have the same NMR-active nucleus.

There is little experimental data about the species that exist at high temperature although it has been proposed that different $[P_xQ_y]^{z-}$ anions exist in the melt in various equilibria [1]. Since there is ^{31}P chemical shift discrimination between P–P and non-P–P bonded selenophosphate species in room temperature solids, *in situ* ^{31}P NMR studies

Abbreviations: CSA; Chemical shift anisotropy; MAS; Magic angle spinning

*Corresponding author. Fax: +1 517 355 1793.
E-mail addresses: m-kanatzidis@northwestern.edu (M.G. Kanatzidis), weliky@chemistry.msu.edu (D.P. Weliky).
[1]Also for correspondence to. Fax: +1 847 491 7713.

0022-4596/$ - see front matter © 2007 Elsevier Inc. All rights reserved.
doi:10.1016/j.jssc.2007.08.002

of high-temperature syntheses can potentially provide information about the identity of ^{31}P-containing species that exist at high temperature. The known compound $Cs_4P_2Se_9$ [13] was initially chosen for a high-temperature NMR study because: (1) the synthesis temperature could be reached by our NMR probe; (2) the compound contained the interesting Se-bridged $[P_2Se_9]^{4-}$ anion; and (3) the compound melts congruently which suggests that spectra of subsequent high-temperature remelts should be similar to one another and that some correlation can be made between the remelt spectra and the spectrum of the solid compound.

In this paper, we present the new compound $Cs_4P_2Se_{10}$ which was discovered following high-temperature *in situ* NMR synthesis intended to produce $Cs_4P_2Se_9$. Room temperature solid-state ^{31}P NMR spectra of the synthetic products clearly showed that $Cs_4P_2Se_9$ was not the dominant crystalline product and the structure of $Cs_4P_2Se_{10}$ was subsequently solved with X-ray diffraction of single crystals obtained from the NMR synthesis. Synthetic conditions were varied to ascertain the important factors leading to dominant $Cs_4P_2Se_9$ or $Cs_4P_2Se_{10}$ products and high-temperature ^{31}P NMR spectra of synthetic melts were obtained and analyzed.

2. Experimental section

2.1. Sample preparation

Chemicals were used as obtained unless otherwise noted: phosphorous (MCB Reagents, Gibbstown, NJ, amorphous red), selenium shot (Tellurex Inc., Traverse City, MI, 99.999%) cesium metal, (Aldrich Chemical Co., Inc., St. Louis, MO). Phosphorous was freeze dried and Cs_2Se was prepared by a modified literature preparation [14,15]. P_2Se_5 was prepared by combining a stoichiometric amount of the elements in a pyrex ampoule, flame-sealing at a reduced pressure of ~100 mTorr, then heating to 300 °C over 6 h, holding there for 6 h, and then quenching in air. Manipulations of all starting materials were performed under a nitrogen atmosphere in a dry box (Vacuum Atmospheres Inc.).

The synthesis that produced $Cs_4P_2Se_{10}$ as the dominant P-containing product was performed by combining Cs_2Se (0.186 g, 0.53 mmol), P_2Se_5 (0.124 g, 0.27 mmol), and Se (0.192 g, 2.4 mmol) which were subsequently ground together in an agate mortar and pestle to increase homogeneity. This resulted in a reaction stoichiometry with the nominal composition "$Cs_4P_2Se_{16}$" or an excess of six equivalents of Se relative to the $Cs_4P_2Se_{10}$ stoichiometry. The extra Se in the reaction stoichiometry was added to favor the production of $Cs_4P_2Se_{10}$ rather than $Cs_4P_2Se_9$ [13]. Approximately 75 mg of this mixture was loaded into a fused silica ampoule, sealed at ~100 mTorr, and placed in the high-temperature NMR probe. The sample was then heated at a rate of 10 °C/min, with pauses in the temperature ramp to collect isothermal NMR spectra. After reaching the maximum temperature of 600 °C and collecting an NMR spectrum, the sample was cooled back to room temperature at a rate of 10 °C/min, again pausing for spectral collection. The total time spent above room temperature was ~6 h. A room temperature ^{31}P NMR spectrum following the *in situ* synthesis contained a dominant isotropic peak at −52.8 ppm and integration of all the spectral peaks indicated that $Cs_4P_2Se_{10}$ was >99% of the total P-containing compounds (Fig. 1A). Powder X-ray diffraction indicated that elemental Se also remained in the final products. It was also possible to prepare $Cs_4P_2Se_{10}$ with a conventional high-temperature furnace using the same stoichiometry and a heating/cooling profile of a similar length. Crystals of $Cs_4P_2Se_{10}$ were air and moisture stable over a period of at least several hours.

$Cs_4P_2Se_9$ was produced in high purity by combining Cs_2Se (0.281 g, 0.82 mmol), P_2Se_5 (0.186 g, 0.41 mmol), and Se (0.032 g, 0.41 mmol) in a fused silica ampoule. This resulted in a "$Cs_4P_2Se_8$" reaction stoichiometry and under these Se starved conditions, $Cs_4P_2Se_9$ is favored. The ampoule was subsequently sealed under a reduced pressure of ~100 mTorr and allowed to react in a furnace. The sample was heated to 700 °C over 12 h, held at 700 °C for 12 h, and then cooled to room temperature over 12 h. The room temperature ^{31}P NMR spectrum had a dominant isotropic peak at −39.9 ppm and integration of all the spectral peaks indicated that $Cs_4P_2Se_9$ was >90% of the

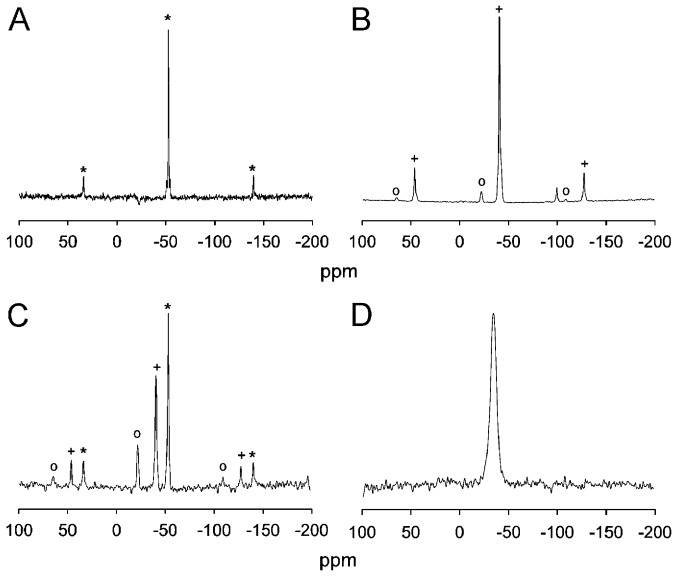

Fig. 1. Ambient temperature ^{31}P MAS NMR spectra of the final products of: (A) a "$Cs_4P_2Se_{16}$" reaction stoichiometry indicating $Cs_4P_2Se_{10}$ as the dominant ^{31}P-containing species at −52.8 ppm; (B) a "$Cs_4P_2Se_8$" reaction stoichiometry indicating $Cs_4P_2Se_9$ as the dominant ^{31}P-containing species at −39.9 ppm; and (C) a "$Cs_4P_2Se_{12}$" reaction stoichiometry that produced $Cs_4P_2Se_9$ and $Cs_4P_2Se_{10}$ in a ~3:5 ratio. Panel D displays the static ^{31}P NMR spectrum of a 350 °C melt of the products in C. The peak with a chemical shift of −22.0 ppm in panels B and C was not assigned and the peak at −99.8 ppm in panel B was not assigned. For spectra A–C, the spinning frequency was 14 kHz and spinning sidebands are grouped with the corresponding isotropic peak using like symbols with *≡$Cs_4P_2Se_{10}$, +≡$Cs_4P_2Se_9$, and o≡unassigned peak with −22.0 ppm isotropic shift.

^{31}P-containing compounds (Fig. 1B). There were also peaks at −22.0 and −99.8 ppm that accounted for the remainder of the spectral intensity but were not assigned. The powder X-ray diffraction pattern contained only peaks that corresponded to $Cs_4P_2Se_9$.

Vitrification of the mixture with "$Cs_4P_2Se_{16}$" stoichiometry was accomplished by sealing a sample portion in a fused silica ampoule under a reduced pressure of ~100 mTorr, flame heating until molten, and then rapidly quenching in ice water. Complete vitrification was confirmed by powder X-ray diffraction.

2.2. Crystallographic studies

Intensity data for single crystals of $Cs_4P_2Se_{10}$ were collected on a Bruker SMART platform CCD diffractometer using Mo$K\alpha$ radiation operating at 40 kV and 40 mA (Table 1). A full sphere of data was collected and individual frames were acquired with a 10 s exposure time and a 0.3° Ω rotation. The SMART software was used for data collection, and SAINT software was used for data extraction and reduction. An analytical absorption correction to the data was performed and direct methods were used to solve and refine the structures with the SHELXTL [16] software package.

Powder X-ray diffraction was performed with a Rigaku-Denki RW400F2 (Rotaflex) diffractometer equipped with a Cu$K\alpha$ rotating anode operating at 45 kV and 100 mA with a 2°/min scan rate.

2.3. NMR spectroscopy

Room temperature ^{31}P NMR spectra were collected on a 9.4 T spectrometer (Varian Infinity Plus) using a magic angle spinning (MAS) probe (Varian Chemagnetics) and served as an analytical tool to assess the phase purity of P-containing compounds. Samples were spun at 7–14 kHz in zirconia rotors of 4 mm outer diameter and a ~50 μL sample volume. Bloch decay spectra were taken with a 4.6 μs $\pi/2$ pulse calibrated using H_3PO_4 which also served as a chemical shift reference at 0 ppm. Four scans were summed with a 5000 s recycle delay. The longitudinal relaxation time of $Cs_4P_2Se_{10}$ at ambient temperature was determined by fitting the signal intensity as a function of relaxation delay to an exponential buildup function [5].

High-temperature ^{31}P NMR spectra were collected on a 9.4 T spectrometer (Varian Infinity Plus) using a static probe (Doty Scientific) with a 5.5 μs $\pi/2$ pulse calibrated at room temperature using H_3PO_4 which also served as a chemical shift reference at 0 ppm. Several hundred to several thousand scans were averaged with recycle delays ranging from 0.1 to 10 s. Sample temperatures ranging from 250 to 600 °C were reached at a rate of 10 °C/min and were allowed to equilibrate for ~5 min before data collection.

All NMR spectra were processed with line broadening and baseline correction.

2.4. Differential thermal analysis (DTA)

DTA was performed on a Shimadzu DTA-50 thermal analyzer. Sample portions (~30 mg) were sealed under a reduced pressure of ~80 mTorr in fused silica, and an equivalent mass of Al_2O_3 in a similarly prepared ampoule served as a reference. The sample was heated to 600 °C at a rate of 10 °C/min and then cooled at a rate of 10 °C/min back to room temperature. The residues after DTA were analyzed by powder X-ray diffraction.

3. Results and discussion

3.1. Identification and structure description of $Cs_4P_2Se_{10}$

The initial goal of synthesizing $Cs_4P_2Se_9$ in a sealed tube in the NMR spectrometer was to obtain high-temperature ^{31}P NMR spectra and to identify species present in the synthetic melt. After one of the syntheses was complete, the room temperature ^{31}P NMR spectrum contained a dominant peak at −52.8 ppm in addition to the −39.9 ppm shift of $Cs_4P_2Se_9$ [11]. The −52.8 ppm peak could not be assigned to any known compound. Single deep reddish brown crystals were isolated, screened using X-ray diffraction, and the structure of $Cs_4P_2Se_{10}$ was subsequently solved. A summary of the details of the refinement are displayed in Table 1. All of the peaks in the powder X-ray diffraction pattern of the sample prepared using the optimized synthetic method corresponded either to the calculated $Cs_4P_2Se_{10}$ pattern or to elemental Se. The ^{31}P NMR peak at −52.8 ppm was therefore assigned to $Cs_4P_2Se_{10}$.

$Cs_4P_2Se_{10}$ has the molecular anion $[P_2Se_{10}]^{4-}$ which is composed of two PSe_4 tetrahedra that are connected by two central selenium atoms thus forming a tetraselenide fragment (Fig. 2A). The PSe_4 tetrahedron is distorted with the Se–P–Se angles ranging from 92.14(9)° to 116.67(10)°. The lengths of the P–Se bonds are typical and range from 2.159(2) to 2.312(2) Å. Tables 2 and 3 contain the atomic

Table 1
Crystallographic data for $Cs_4P_2Se_{10}$

Formula	$Cs_4P_2Se_{10}$	d_{calc} (g/cm^3)	4.153
FW	1383.18	μ (mm^{-1})	23.113
Space group	P-1	λ (Å)	0.71073
a (Å)	7.3587(11)	Temp (K)	298
b (Å)	7.4546(11)	$2\theta_{max}$ (deg)	56.6
c (Å)	10.1420(15)	R^a ($I>2\sigma(I)$)	$R1 = 0.0395$
α (deg)	85.938(2)		w$R2 = 0.0716$
β (deg)	88.055(2)	R^a (all)	$R1 = 0.0687$
γ (deg)	85.609(2)		w$R2 = 0.0789$
V (Å^3)	553.10(14)		
Z	1		

[a] $R = \Sigma(|F_o|-|F_c|)/\Sigma|F_o|$. $Rw = [\Sigma w(|F_o|-|F_c|)^2/\Sigma w|F_o|^2]^{1/2}$.

and thermal parameters, and selected bond lengths and angles, respectively.

The Se–Se contacts range from 2.3125(13) to 2.4045(19) Å, a large range of bond lengths. This unusual behavior could be explained by the dihedral angles [17] around the bonds Se(4)–Se(5) and Se(5)–Se(5) of −83.78(1)° and 180.00(1)°, respectively. It is noteworthy that the Se(5)–Se(5) bond is shared by two planar structural moieties, namely Se(4)–Se(5)–Se(5)–Se(4) and Se(2)···Se(5)–Se(5)···Se(2) to give maximized lone pair repulsion in Se atoms and one of the longest Se–Se distances reported for a selenophosphate ligand. Comparable or even longer Se–Se distances have been found in the Se_n^{2-} ($n = 2$, 3) subunits in the K_2Se_2, Rb_2Se_2 [18], $Sr_4Sn_2Se_9$, $Sr_4Sn_2Se_{10}$ [19] and $Eu_8(Sn_4Se_{14})(Se_3)_2$ [20]. A bond distance alteration in Q_4^{2-} ($Q = S$, Se) has been reported in $Cs_4P_2S_{10}$ [21], $APSe_6$ ($A = K$, Rb, Cs) [22], and unligated Se_4^{2-} ions [23].

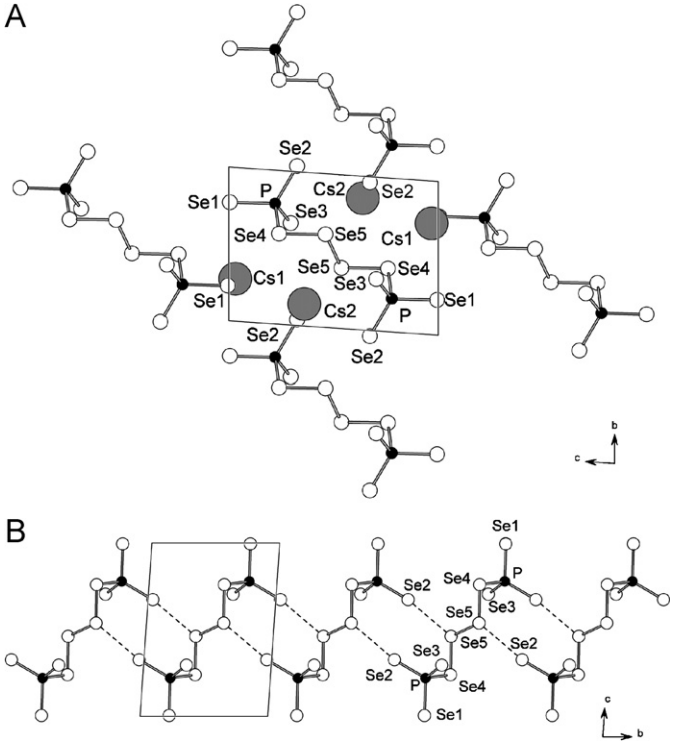

Fig. 2. Structure of $Cs_4P_2Se_{10}$ (A) down the *a*-axis showing the $[P_2Se_{10}]^{4-}$ chains and (B) along the *b*-axis with the weak interaction between the $[P_2Se_{10}]^{4-}$ chains emphasized with a dashed line.

For $Cs_4P_2Se_{10}$, unusually short intra- and intermolecular Se···Se nonbonding interactions are observed at 3.243(4) and 3.399(4) Å. Intermolecular nonbonding interactions generate a pseudo-one-dimensional infinite chain including eight-membered rings composed of P and Se atoms along the *b*-axis (Fig. 2B).

The structure of $Cs_4P_2Se_{10}$ is related to the structure of $Cs_4P_2S_{10}$ [21] and both contain the $[P_2Q_{10}]^{4-}$ anion. In $Cs_4P_2S_{10}$, there are two different conformations of the $[P_2S_{10}]^{4-}$ anion with dihedral angles about the central disulfide bonds of 89.6° and 0°. In $Cs_4P_2Se_{10}$, only one anionic conformation is present with a dihedral angle about the central diselenide bond of 180° (vide supra). Additionally, there is positional disorder of the S atoms in $Cs_4P_2S_{10}$, and this is not evident for the Se atoms in $Cs_4P_2Se_{10}$.

3.2. Differential thermal analysis (DTA)

For the glass with "$Cs_4P_2Se_{16}$" stoichiometry, the first DTA heating cycle indicated an exothermic crystallization event centered at ~160 °C and broad endothermic melting features centered at 315 °C. The subsequent cooling cycle contained exothermic crystallization features that were centered near 275 °C. Subsequent DTA cycles were similar to the first cycle except that they did not contain the initial crystallization peak near 160 °C. Possible assignments of the DTA features are: (1) 160 °C exothermic feature, glass to crystal phase transition of $Cs_4P_2Se_{10}$ and Se; (2) 315 °C endothermic feature/275 °C exothermic features, melting/crystallization of $Cs_4P_2Se_{10}$ and Se.

The assignment of the 160 °C feature is supported by several arguments. First, the feature is exothermic and is only observed during the first heating cycle as would be expected for a transition from a metastable glass to a thermodynamically stable crystal. Second, annealing the glass near the putative glass to crystal transition temperature resulted in formation of a mixture of crystalline materials that were predominantly $Cs_4P_2Se_{10}$ and Se. ^{31}P solid state NMR and powder X-ray diffraction were the methods used to analyze the annealed material. The glass to crystal transition temperature of the $Cs_4P_2Se_{16}$ glass is

Table 2
Fractional atomic coordinates and anisotropic thermal parameters for $Cs_4P_2Se_{10}$ with standard deviations in parentheses

Atom	*x*	*y*	*z*	U_{11}	U_{22}	U_{33}	U_{12}	U_{13}	U_{23}
Cs1	0.2210(1)	0.2754(1)	0.9686(1)	0.0178(3)	0.0178(3)	0.0206(3)	−0.0030(2)	0.0010(2)	−0.0035(2)
Cs2	0.1943(1)	−0.1431(1)	1.3603(1)	0.0272(4)	0.0328(4)	0.0192(3)	0.0120(3)	−0.0038(3)	−0.0012(3)
Se1	0.2682(1)	0.7719(1)	0.9946(1)	0.0180(5)	0.0190(5)	0.0110(4)	−0.0009(4)	0.0001(4)	0.0003(4)
Se2	0.3081(1)	0.0372(1)	0.6737(1)	0.0256(5)	0.0139(5)	0.0173(5)	−0.0040(4)	0.0014(4)	0.0026(4)
Se3	0.0229(1)	0.6635(1)	0.7046(1)	0.0154(5)	0.0231(5)	0.0192(5)	−0.0050(4)	-0.0028(4)	−0.0008(4)
Se4	0.5116(1)	0.5897(1)	0.7599(1)	0.0156(5)	0.0206(5)	0.0115(4)	0.0031(4)	−0.0017(4)	−0.0003(4)
Se5	0.4017(1)	-0.6057(1)	1.4616(1)	0.0216(5)	0.0191(5)	0.0150(5)	−0.0030(4)	0.0041(4)	0.0001(4)
P	0.2533(3)	0.7841(3)	0.7789(2)	0.0122(11)	0.0126(11)	0.0112(11)	0.0005(8)	0.0007(9)	−0.0002(9)

Table 3
Selected bond lengths (Å) and angles (deg) for $Cs_4P_2Se_6$ with standard uncertainties in parentheses

Cs1–Se2	3.5999(12)	Se2–Cs1–Se1^{i}	98.40(2)	Se5–Cs2–Se1^{iii}	91.31(2)
Cs1–Se1^{i}	3.6487(12)	Se2–Cs1–Se4^{ii}	136.97(3)	Se2^{vi}–Cs2–Se1^{iii}	82.20(2)
Cs1–Se4^{ii}	3.6769(11)	Se1^{i}–Cs1–Se4^{ii}	121.94(3)	Se2^{iv}–Cs2–Se5^{vii}	64.72(2)
Cs1–Se1^{iii}	3.7348(12)	Se2–Cs1–Se1^{iii}	60.58(2)	Se2^{v}–Cs2–Se5^{vii}	150.79(3)
Cs1–Se3^{i}	3.7543(12)	Se1^{i}–Cs1–Se1^{iii}	85.52(2)	Se5–Cs2–Se5^{vii}	36.99(3)
Cs1–Se1	3.7718(12)	Se4^{ii}–Cs1–Se1^{iii}	105.05(2)	Se2^{vi}–Cs2–Se5^{vii}	52.92(2)
Cs1–Se1^{ii}	3.7762(12)	Se2–Cs1–Se3^{i}	151.36(3)	Se1^{iii}–Cs2–Se5^{vii}	106.06(2)
Cs1–Se4	3.7815(11)	Se1^{i}–Cs1–Se3^{i}	59.45(2)	Se2^{iv}–Cs2–Se3^{i}	81.89(2)
Cs1–Se3	4.0230(12)	Se4^{ii}–Cs1–Se3^{i}	62.58(2)	Se2^{v}–Cs2–Se3^{i}	56.86(2)
		Se1^{iii}–Cs1–Se3^{i}	97.29(2)	Se5–Cs2–Se3^{i}	174.05(3)
Cs2–Se2^{iv}	3.6835(12)	Se2–Cs1–Se1	125.33(3)	Se2^{vi}–Cs2–Se3^{i}	98.24(3)
Cs2–Se2^{v}	3.7433(12)	Se1^{i}–Cs1–Se1	104.42(2)	Se1^{iii}–Cs2–Se3^{i}	94.65(2)
Cs2–Se5	3.7522(12)	Se4^{ii}–Cs1–Se1	62.04(2)	Se5^{vii}–Cs2–Se3^{i}	140.01(3)
Cs2–Se2^{vi}	3.8038(13)	Se1^{iii}–Cs1–Se1	166.51(3)	Se2^{iv}–Cs2–Se3^{viii}	56.76(2)
Cs2–Se1^{iii}	3.8210(12)	Se3^{i}–Cs1–Se1	80.51(2)	Se2^{v}–Cs2–Se3^{viii}	80.29(2)
Cs2–Se5^{vii}	3.8251(12)	Se2–Cs1–Se1^{ii}	85.58(2)	Se5–Cs2–Se3^{viii}	65.82(2)
Cs2–Se3^{i}	3.8256(12)	Se1^{i}–Cs1–Se1^{ii}	164.68(3)	Se2^{vi}–Cs2–Se3^{viii}	117.21(2)
Cs2–Se3^{viii}	3.8891(12)	Se4^{ii}–Cs1–Se1^{ii}	51.56(2)	Se1^{iii}–Cs2–Se3^{viii}	145.71(3)
Cs2–Se4^{vi}	4.0678(12)	Se1^{iii}–Cs1–Se1^{ii}	83.59(2)	Se5^{vii}–Cs2–Se3^{viii}	71.46(2)
		Se3^{i}–Cs1–Se1^{ii}	111.37(2)	Se3^{i}–Cs2–Se3^{viii}	108.89(2)
Se1–P	2.190(2)	Se1–Cs1–Se1^{ii}	84.84(2)	Se2^{iv}–Cs2–Se4^{vi}	118.71(3)
Se2–P^{iii}	2.159(2)	Se2–Cs1–Se4	77.82(2)	Se2^{v}–Cs2–Se4^{vi}	126.19(3)
Se3–P	2.160(2)	Se1^{i}–Cs1–Se4	134.20(3)	Se5–Cs2–Se4^{vi}	34.10(2)
Se4–P	2.312(2)	Se4^{ii}–Cs1–Se4	83.33(2)	Se2^{vi}–Cs2–Se4^{vi}	72.12(2)
		Se1^{iii}–Cs1–Se4	127.31(2)	Se1^{iii}–Cs2–Se4^{vi}	58.15(2)
Se4–Se5^{vi}	2.3125(13)	Se3^{i}–Cs1–Se4	130.32(3)	Se5^{vii}–Cs2–Se4^{vi}	54.02(2)
Se5–Se5^{vii}	2.4045(19)	Se1–Cs1–Se4	50.85(2)	Se3^{i}–Cs2–Se4^{vi}	151.64(3)
		Se1^{ii}–Cs1–Se4	61.07(2)	Se3^{viii}–Cs2–Se4^{vi}	99.08(2)
		Se2–Cs1–Se3	81.70(3)	Se4^{vi}–Se5–Se5^{vii}	99.15(6)
		Se1^{i}–Cs1–Se3	78.51(2)	Se2^{ix}–P–Se3	113.11(10)
		Se4^{ii}–Cs1–Se3	118.03(3)	Se2^{ix}–P–Se1	116.67(10)
		Se1^{iii}–Cs1–Se3	136.25(3)	Se3–P–Se1	115.17(10)
		Se3^{i}–Cs1–Se3	108.52(2)	Se2^{ix}–P–Se4	107.73(10)
		Se1–Cs1–Se3	56.10(2)	Se3–P–Se4	109.49(10)
		Se1^{ii}–Cs1–Se3	116.77(2)	Se1–P–Se4	92.14(9)
		Se4–Cs1–Se3	55.71(2)		
		Se2^{iv}–Cs2–Se2^{v}	105.69(2)	Se3–P–Cs1	71.49(6)
		Se2^{iv}–Cs2–Se5	92.66(3)	Se1–P–Cs1	64.65(6)
		Se2^{v}–Cs2–Se5	123.04(3)	Se4–P–Cs1	64.51(6)
		Se2^{iv}–Cs2–Se2^{vi}	73.48(3)	Se2^{ix}–P–Cs1^{ix}	57.99(6)
		Se2^{v}–Cs2–Se2^{vi}	154.34(3)	Se3–P–Cs1^{ix}	124.72(8)
		Se5–Cs2–Se2^{vi}	82.40(2)	Se1–P–Cs1^{ix}	61.53(6)
		Se2^{iv}–Cs2–Se1^{iii}	154.59(3)	Se4–P–Cs1^{ix}	125.46(8)
		Se2^{v}–Cs2–Se1^{iii}	93.00(2)	Cs1–P–Cs1^{ix}	125.30(6)

(i) $-x, 1-y, 2-z$; (ii) $1-x, 1-y, 2-z$; (iii) $x, -1+y, z$; (iv) $x, y, 1+z$; (v) $-x, -y, 2-z$; (vi) $1-x, -y, 2-z$; (vii) $1-x, -1-y, 3-z$; (viii) $x, -1+y, 1+z$; (ix) $x, 1+y, z$.

lower than the corresponding temperatures that have been observed for glasses that form related metal selenophosphate compounds [22,24,25]. Materials with a reversible glass to crystal phase transition have potential use in data storage applications [22,26–30], and further characterization of the phase change properties of $Cs_4P_2Se_{10}$ may be of technological relevance.

3.3. Competition between $Cs_4P_2Se_9$ and $Cs_4P_2Se_{10}$

Analysis of the products of furnace reactions done with different stoichiometries showed that reaction stoichiometry had a significant effect on the $Cs_4P_2Se_{10}$:$Cs_4P_2Se_9$ final product ratio. Reduction by one equivalent of Se relative to $Cs_4P_2Se_9$, i.e. "$Cs_4P_2Se_8$" reaction stoichiometry, produced $Cs_4P_2Se_9$ as the dominant ^{31}P-containing product with no $Cs_4P_2Se_{10}$, Fig. 1B. Syntheses with increased Se relative to $Cs_4P_2Se_{10}$, i.e. "$Cs_4P_2Se_{10+x}$" with $1<x<5$ reaction stoichiometries, resulted in mixtures of $Cs_4P_2Se_9$ and $Cs_4P_2Se_{10}$. A representative spectrum of the products of the reaction where $x=2$ is displayed in Fig. 1C. For the "$Cs_4P_2Se_{16}$" reaction stoichiometry, $Cs_4P_2Se_{10}$ was the only P-containing compound (Fig. 1A). The Fig. 1B,C spectra also had small peaks at −22.0 and −99.8 ppm that accounted for <10% of the total ^{31}P signal intensity. To our knowledge, these shifts do not correspond to the measured ^{31}P shifts of any known cesium selenophosphate compound. The related compound $Cs_4P_2S_{10}$

was synthesized with the "$Cs_4P_2S_{10.5}$" reaction stoichiometry and although there was excess S, the as-yet unknown compound $Cs_4P_2S_9$ was not produced [21].

The literature preparation of $Cs_4P_2Se_9$ was done with the "$Cs_{5.4}P_2Se_{13.4}$" reaction stoichiometry that contained an excess of both Cs and Se relative to $Cs_4P_2Se_9$ [13]. Although an excess of elemental Se in the present study was found to favor the production of $Cs_4P_2Se_{10}$, this effect appeared to be counteracted in the literature preparation by an increased Se^{2-}/Se ratio that was a result of the excess Cs_2Se. The Se^{2-}/Se ratio correlates with the negative charge/Se atom ratio in the melt and increasing these ratios might reasonably favor selenophosphate anions with shorter Se chains [31].

Experiments were also done to understand the effect of the length of the heating/cooling profile on the $Cs_4P_2Se_{10}$/$Cs_4P_2Se_9$ crystalline product ratio. The 600 °C furnace syntheses were done with a "$Cs_4P_2Se_{12}$" reaction stoichiometry and the heating/cooling profile length was varied between 18 and 54 h. For all profile lengths, the final product distribution showed that $Cs_4P_2Se_{10}$ was more abundant than $Cs_4P_2Se_9$ but there was a general trend towards smaller $Cs_4P_2Se_{10}$:$Cs_4P_2Se_9$ ratios with longer heating/cooling profiles. This effect may provide some explanation for the discovery of $Cs_4P_2Se_{10}$ under the relatively short 6 h heating/cooling profile of the initial NMR syntheses.

3.4. ^{31}P room temperature and high-temperature NMR spectroscopy

A Herzfeld–Berger analysis [32] of a room temperature ^{31}P NMR spectrum of $Cs_4P_2Se_{10}$ taken at 7 kHz spinning frequency indicated δ_{11}, δ_{22}, and δ_{33} chemical shift anisotropy (CSA) principal values of 50, −41, and −167 ppm, respectively, [33] and similar values were obtained at 12 kHz spinning frequency. The $\delta_{11}-\delta_{33}$ CSA principal value difference of ~215 ppm was comparable to that of $Cs_4P_2Se_9$ (~180 ppm) and other compounds with $[P_xSe_y]^{z-}$ anions containing $(Se–Se)_n$ linkages [11]. The longitudinal relaxation time T_1 of $Cs_4P_2Se_{10}$ was 2100 ± 600 s and was comparable to the T_1 values of other metal selenophosphate compounds [5]. For both $Cs_4P_2Se_9$ and $Cs_4P_2Se_{10}$ peaks, splittings were observed corresponding to P–Se spin–spin coupling with coupling constant of ~270 Hz.

The high-temperature ^{31}P NMR spectra of the melts of syntheses that produced $Cs_4P_2Se_{10}$ or $Cs_4P_2Se_{10}$/$Cs_4P_2Se_9$ mixtures contained one peak. Fig. 1D displays a representative spectrum of a 350 °C melt formed from $Cs_4P_2Se_9$:$Cs_4P_2Se_{10}$ products in a 3:5 ratio (Fig. 1C). Spectra obtained at a given temperature were independent of both the direction of the temperature ramp and the thermal history of the sample.

Although analysis of these spectra is not yet complete, some general spectral interpretation is presented. The −35 ppm shift at 350 °C was consistent with room temperature chemical shifts of compounds with non-P–P bonded selenophosphate anions and suggested that the P-containing high-temperature species did not contain P–P bonds [11]. The high temperature shift was more positive than the crystalline $Cs_4P_2Se_9$ or $Cs_4P_2Se_{10}$ shifts observed at room temperature perhaps because of the loss of defined Cs^+ ion coordination. An alternate interpretation is that the ^{31}P-containing species at high-temperature were neither the $[P_2Se_9]^{4-}$ nor the $[P_2Se_{10}]^{4-}$ anions. At room temperature, the shifts of $Cs_4P_2Se_9$ and $Cs_4P_2Se_{10}$ differ by 13 ppm and it might be expected that if both $[P_2Se_9]^{4-}$ and $[P_2Se_{10}]^{4-}$ anions existed in high concentrations at high temperature, two peaks would be observed in the high-temperature spectrum. However, only one peak was observed in all of the melts. The presence of two peaks in the room temperature spectrum but only one peak in the high- temperature spectrum (Fig. 1C,D) shows that there is not a clear NMR correlation between speciation in the crystalline products and speciation in the high- temperature melt. It is possible that fast chemical exchange at high temperature prevented observation of discrete chemical shifts for the different species; however, such chemical exchange was not obvious. The final product spectra indicated an increase in the $Cs_4P_2Se_{10}$:$Cs_4P_2Se_9$ ratio with increasing Se but there was no clear trend of the ^{31}P chemical shift in the high-temperature melts as a function of Se stoichioimetry. For a single temperature, the overall chemical shift variation in the melts as a function of stoichiometry was less than 10 ppm. In the future, spectra could be obtained at lower temperatures and broader linewidths at these temperatures would provide evidence for chemical exchange.

The peak widths of the ^{31}P NMR spectra at 350 °C were typically ~7 ppm or ~1 kHz which was less than the CSA magnitudes of $Cs_4P_2Se_{10}$ (~215 ppm, 35 kHz) and $Cs_4P_2Se_9$ (~180 ppm, 30 kHz) [11]. The relative sharpness of the line at high temperature indicated that most of the anisotropy had been averaged out by random tumbling. Therefore, the frequency of motion must be >30 kHz, or have a rotational correlation time of <5 μs/rad [34]. In the context of the Stokes–Einstein–Debye equation for a sphere tumbling in a liquid, this correlation time τ is proportional to the viscosity η and is inversely proportional to the sphere volume V:

$$\tau = \frac{\eta}{k_B T V}, \quad (1)$$

where k_B is the Boltzmann constant and T is temperature in K units [35]. Using a known T and estimated τ, Eq. (1) could be used to calculate either η or V given a value for the complementary property. Although neither η nor V in selenophosphate melts is known with certainty, there is some information to assess these quantities: (1) flame-heated melts readily flow when the sample tube is inverted; and (2) the P-containing species are likely small molecular rather than large polymeric species because the final crystalline products contain discrete $[P_2Se_9]^{4-}$ or

$[P_2Se_{10}]^{4-}$ anions. In the next paragraph, (1) V is estimated from the dimensions of the $[P_2Se_{10}]^{4-}$ anion; (2) η is calculated using this value of V; and (3) comparison is made between this calculated η and visual assessment of the melt viscosity. This approach tests whether a viscosity calculated with the assumption of small P-containing anions is close to the viscosity estimated from visual observation of the melts.

The radius of the $[P_2Se_{10}]^{4-}$ anion was estimated to be $r \approx 8$ Å from the longest Se–Se distance within a single $[P_2Se_{10}]^{4-}$ anion and the Se^{2-} ionic radius. Using $V = 4\pi r^3/3$, $T = 1000$ K (estimated temperature of flame-heated melt), and $\tau = 5\,\mu s$, Eq. (1) yielded $\eta \sim 15$ Pa*s which is comparable to the viscosity of honey at room temperature[36] or glycerol at 0 °C [37]. This calculated η is likely an upper limit because $\tau = 5\,\mu s$ is an upper limit and because the P-containing anions might be smaller than $[P_2Se_{10}]^{4-}$, e.g. $[PSe_4]^{3-}$ with corresponding smaller V. Despite these caveats, there is general consistency between the calculated η and visual observation of the melt viscosity. The approach therefore yields qualitative support for the existence of small P-containing species [22]. For comparative purposes, the viscosity of liquid Se at 350 °C is 0.07 Pa*s [38].

4. Concluding remarks

The *in situ* NMR synthesis targeting $Cs_4P_2Se_9$ led to the discovery of $Cs_4P_2Se_{10}$ which can be formed with excess Se and a rapid heating/cooling profile. The $Cs_4P_2Se_{10}$ structure contained the novel discrete molecular anion $[P_2Se_{10}]^{4-}$. The chemically related compound $Cs_4P_2S_{10}$ is non-isomorphic, and it is possible that there are multiple polymorphs of both the thio- and seleno-compounds. The optimum $Cs_4P_2Se_{10}$ synthesis was performed in the high-temperature NMR probe with an excess of Se relative to $Cs_4P_2Se_{10}$ and with a ~6 h heating/cooling profile. The $Cs_4P_2Se_{10}$:$Cs_4P_2Se_9$ final product ratio from furnace syntheses was dependent on stoichiometry and on the length of the heating/cooling profile. $Cs_4P_2Se_9$ and $Cs_4P_2Se_{10}$ were favored with Se-starved and Se-rich stoichiometries and with long and short heating/cooling profiles, respectively.

Room temperature ^{31}P NMR spectra provided a facile means of evaluating the relative amounts of the P-containing compounds made in furnace and NMR syntheses. In addition, some of these spectra presented in the paper have peaks that have not yet been assigned to known crystalline compounds. Careful screening of crystals from these reactions may therefore result in new compound identification.

The high-temperature static ^{31}P NMR spectra of the synthetic melts contained one relatively narrow peak that may be the result of a rapidly tumbling selenophosphate anion that does not contain P–P bonds, i.e. a P^{5+} species. Future time-dependent studies of high-temperature spectra may provide information about reaction rates. As illustrated by the discovery of $Cs_4P_2Se_{10}$, future high-temperature NMR syntheses may also aid discovery of new compounds.

5. Supplemental data

A DTA plot and a ^{31}P NMR spectrum with 7 kHz MAS frequency are included. Further details of the $Cs_4P_2Se_{10}$ crystal structure investigation can be obtained from the Fachinformationszentrum Karlsruhe, 76344 Eggenstein-Leopoldshafen, Germany, (fax: +49 7247 808 666; email: crysdata@fiz.karlsruhe.de) on quoting the depository number CSD 418434.

Acknowledgments

We acknowledge financial support from the National Science Foundation (Grant DMR-0443785) and Tellurex Inc. for the gift of Se metal.

Appendix A. Supporting information

Supplementary data associated with this article can be found in the online version at doi:10.1016/j.jssc.2007.08.002.

References

[1] M.G. Kanatzidis, Curr. Opin. Solid State Mater. 2 (1997) 139–149.
[2] P. Bridenbaugh, Mater. Res. Bull. 8 (1973) 1055–1060.
[3] E.D. Rogach, E.V. Sviridov, E.A. Arnautova, E.A. Savchenko, N.P. Protsenko, Zh. Tekh. Fiz. 61 (1991) 201–204.
[4] C.D. Carpentier, R. Nitsche, Mater. Res. Bull. 9 (1974) 1097–1100.
[5] C.G. Canlas, R.B. Muthukumaran, M.G. Kanatzidis, D.P. Weliky, Solid State Nucl. Magn. Reson. 24 (2003) 110–122.
[6] R. Maxwell, H. Eckert, J. Am. Chem. Soc. 115 (1993) 4747–4753.
[7] R. Maxwell, H. Eckert, J. Am. Chem. Soc. 116 (1994) 682–689.
[8] R. Maxwell, H. Eckert, J. Phys. Chem. 99 (1995) 4768–4778.
[9] P.F. Mutolo, M. Witschas, G. Regelsky, J.S.A.D. Guenne, H. Eckert, J. Non-Cryst. Solids 257 (1999) 63–72.
[10] A.J. Schmedt, K. Meise-Gresch, H. Eckert, W. Holand, V. Rheinberger, Glass Sci. Technol. 73 (2000) 90–97.
[11] C.G. Canlas, M.G. Kanatzidis, D.P. Weliky, Inorg. Chem. 42 (2003) 3399–3405.
[12] R.K. Harris, Nuclear Magnetic Resonance Spectroscopy, Longman Scientific and Technical, New York, 1983, p. 18.
[13] K. Chondroudis, M.G. Kanatzidis, Inorg. Chem. 34 (1995) 5401–5402.
[14] F. Fehér, Handbuch der Präparativen Anorganischen Chemie, vol. 1, Ferdinand Enke Verlag, Stuttgart, Germany, 1954, pp. 280–281.
[15] T.J. McCarthy, M.G. Kanatzidis, Inorg. Chem. 34 (1995) 1257–1267.
[16] SHELXTL V-5, Bruker Analytical X-ray Instruments, Inc., Madison, 1998.
[17] A. Hordvik, Acta Chem. Scand. 20 (1966) 1885–1891.
[18] P. Bottcher, J. Getzschmann, R. Keller, Z. Anorg. Allg. Chem. 619 (1993) 476–488.
[19] R. Pocha, D. Johrendt, Inorg. Chem. 43 (2004) 6830–6837.
[20] C.R. Evenson, P.K. Dorhout, Z. Anorg. Allg. Chem. 627 (2001) 2178–2182.
[21] J.A. Aitken, C. Canlas, D.P. Weliky, M.G. Kanatzidis, Inorg. Chem. 40 (2001) 6496–6498.

[22] I. Chung, J. Do, C.G. Canlas, D.P. Weliky, M.G. Kanatzidis, Inorg. Chem. 43 (2004) 2762–2764.
[23] N.E. Brese, C.R. Randall, J.A. Ibers, Inorg. Chem. 27 (1988) 940–943.
[24] J.B. Wachter, K. Chrissafis, V. Petkov, C.D. Malliakas, D. Bilc, T. Kyratsi, K.M. Paraskevopoulos, S.D. Mahanti, T. Torbrugge, H. Eckert, M.G. Kanatzidis, J. Solid State Chem. 180 (2007) 420–431.
[25] K. Chrissafis, T. Kyratsi, K.M. Paraskevopoulos, M.G. Kanatzidis, Chem. Mater. 16 (2004) 1932–1937.
[26] L. Hesselink, A. Mijiritskii (Eds.), Advanced Data Storage Materials and Characterization Techniques, MRS Proceedings, 2003, p. 803.
[27] A.H. Edwards, A.C. Pineda, P.A. Schultz, M.G. Martin, A.P. Thompson, H.P. Hjalmarson, J. Phys.: Condens. Matter 17 (2005) L329–L335.
[28] D.H. Ahn, D.H. Kang, B.K. Cheong, H.S. Kwon, M.H. Kwon, T.Y. Lee, J.H. Jeong, T.S. Lee, I.H. Kim, K.B. Kim, IEEE Electr. Device L. 26 (2005) 286–288.
[29] S. Gidon, O. Lemonnier, B. Rolland, O. Bichet, C. Dressler, Y. Samson, Appl. Phys. Lett. 85 (2004) 6392–6394.
[30] T. Ohta, J. Optoelectron Adv. Mater. 3 (2001) 609–626.
[31] M.G. Kanatzidis, A.C. Sutorik, Prog. Inorg. Chem. 43 (1995) 151–265.
[32] J. Herzfeld, A.E. Berger, J. Chem. Phys. 73 (1980) 6021–6030.
[33] K. Eichele, R.E. Wasylishen, HBA 1.5, Dalhousie University and Universität Tübingen, 2006.
[34] R.K. Harris, Nuclear Magnetic Resonance Spectroscopy, Longman Scientific and Technical, New York, 1983, p. 86.
[35] J. Cavanagh, W. Fairbrother, A. Palmer III, N. Skelton, Protein NMR Spectroscopy: Principles and Practice, Academic Press, San Diego, 1996, pp. 17–19.
[36] L. Juszczak, T. Fortuna, J. Food Eng. 75 (2006) 43–49.
[37] R.C. Weast, M.J. Astle (Eds.), CRC Handbook of Chemistry and Physics, 60th ed., CRC Press Inc. Boca Raton, FL, 1980, p. F-55.
[38] D.E. Harrison, J. Chem. Phys. 41 (1964) 844–849.

Supplemental Data

$Cs_4P_2Se_{10}$: A New Compound Discovered with the Application of Solid State and High Temperature NMR

Matthew A. Gave[a], Christian G. Canlas[a], In Chung[a,b], Ratnasabapathy G. Iyer[a], Mercouri G. Kanatzidis[a,b,*], David P. Weliky[a,*]

weliky@chemistry.msu.edu
m-kanatzidis@northwestern.edu

[a] *Department of Chemistry, Michigan State University, East Lansing, MI, 48824, telephone 517-355-9715, fax 517-355-1793*

[b] *Department of Chemistry, Northwestern University, Evanston, IL, 60208, telephone 847-467-1541, fax 847-491-7713*

**Corresponding Authors*

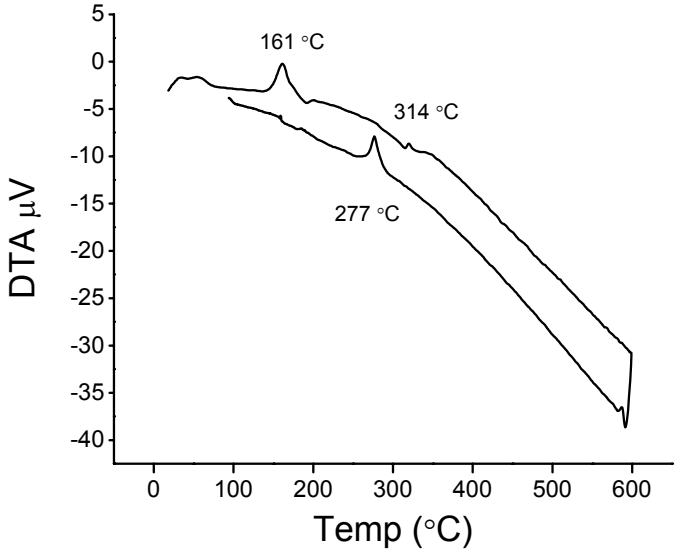

Figure S1. Differential thermal analysis (DTA) of a mixture with "$Cs_4P_2Se_{16}$" stoichiometry that was quenched rapidly from the melt. The displayed plot is for the first heating/cooling cycle of this mixture. The interpretation of this plot relied on the powder X-ray diffraction pattern obtained following several heating/cooling cycles. This pattern indicated that $Cs_4P_2Se_{10}$ and elemental Se were the major crystalline products. In the displayed plot, the peak centered at ~160 ºC is assigned to the glass to crystalline transition of $Cs_4P_2Se_{10}$ and Se, the peak centered at at ~315 ºC is assigned to the melting of this mixture, and the peak centered at 277 ºC is assigned to the subsequent recrystallization. The exothermic peak centered at ~160 ºC was not observed for the second and subsequent heating/cooling cycles likely because the cooling rate was slow enough that crystalline rather than glassy material was formed. Thermal events due to pure Se were not observed perhaps because of insufficient Se or because of comelting/cocrystallization of Se with $Cs_4P_2Se_{10}$.

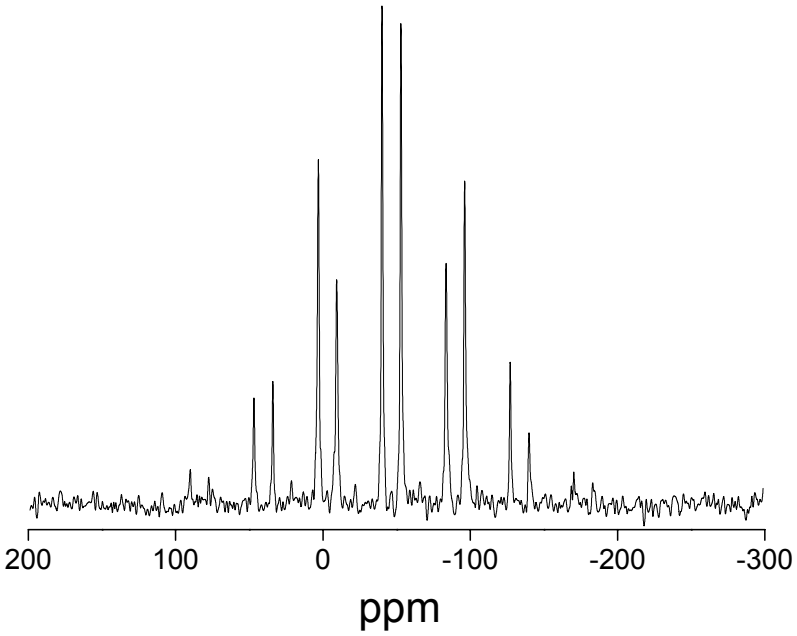

Figure S2. Room temperature ^{31}P NMR spectrum of a reaction that resulted in a mixture of $Cs_4P_2Se_{10}$ and $Cs_4P_2Se_9$. The MAS frequency was 7 kHz. The intensities of peaks corresponding to $Cs_4P_2Se_{10}$ were used for the determination of CSA principal values of this compound.